

# $\nu$ production in Centaurus A and M87 from $\gamma$ -ray interactions with the gas and dust at the sources

J.C. Arteaga-Velázquez

*Instituto de Física y Matemáticas, Universidad Michoacana, Edificio C3, Cd. Universitaria,  
58040 Morelia, Michoacan, Mexico*  
Email: arteaga@ifm.umich.mx

## Abstract

Centaurus A and M87 are the closest galaxies with active galactic nuclei and TeV  $\gamma$ -ray emission. The existence of such TeV radiation suggests the production of a neutrino flux from the photo-hadronic interactions of the  $\gamma$ -photons of the active galaxies and their own gas and dust content. Using a simple model of Centaurus A and M87, the corresponding  $\nu$  luminosities at source and their fluxes at Earth were calculated. The neutrino fluxes associated with the aforementioned process resulted to be  $E^2\Phi_{\nu+\bar{\nu}} \lesssim 10^{-13} \text{ s}^{-1} \text{ GeV cm}^{-2}$ , more than 6 orders of magnitude below the modern upper limits from neutrino telescopes. It will be shown that, at high-energies relevant for neutrino astronomy, these  $\nu$  fluxes are not competitive with those fluxes which could be produced from astrophysical scenarios involving cosmic ray acceleration.

*Keywords:* Centaurus A, M87, Neutrinos, TeV  $\gamma$ -rays

*This is an author-created, un-copyedited version of an article published in Journal of Physics: Conference Series. IOP Publishing Ltd is not responsible for any errors or omissions in this version of the manuscript or any version derived from it. The definitive published authenticated version is available online at doi:10.1088/1742-6596/378/1/012005.*

## 1 Introduction

Centaurus A and M87 are two giant elliptical radio galaxies, which are classified as Fanaroff-Riley I (FR I) type sources [1]. Centaurus A, also known as NGC 5128, is located at a distance of 3.4 Mpc from the Earth [2]. Meanwhile, M87 is some 16.7 Mpc away [3]. These galaxies host the closest active galactic nuclei to the Earth and are the sources of high-energy radiation in the form of TeV  $\gamma$ -rays [4]-[11]. Recently, the Pierre Auger observatory (PAO) detected some ultrahigh-energy cosmic ray (UHECR) events within  $3.1^\circ$  around the direction of Centaurus A [12]. Besides, the PAO showed a weak correlation between the arrival direction of cosmic rays with energies above  $6 \times 10^{19} \text{ eV}$  and the distribution of AGN's [12]. Both PAO's results suggest, in this way, that Centaurus A and M87 could also be the production place of UHECR.

The presence of high-energy gamma- and cosmic rays in Centaurus A and M87 would imply the existence of an associated flux of high-energy neutrinos produced from the interactions of both types of high-energy radiation with the ambient gas and photons of the corresponding galaxies. For the case of UHECR,  $\nu$  production mediated by pion photoproduction has been widely studied in the literature (see, for example, [13, 14, 15, 16]) and its contribution is thought to be the main mechanism of  $\nu$  emission. However, it remains to be proved beyond any reasonable doubt that UHECR are produced in Centaurus A and M87 to guarantee the production of neutrinos from the above process. On the other hand, although it is known that several AGN's are  $\gamma$ -ray emitters, the mechanisms of neutrino production induced by  $\gamma$ -ray collisions [17, 18, 19] in that context are scarcely studied, mainly because they are not expected to produce important  $\nu$  fluxes due to their low cross sections. In any case, these secondary processes should be also contributing to the production of high-energy neutrinos in active galaxies. In the present work, one of such  $\nu$  production mechanisms is studied: the photo-hadronic interaction of gamma-rays with the gas and dust content of active galaxies, in particular, for NGC5128 and M87, assuming that the gamma sources are located at the core of their AGN's<sup>1</sup>. Accordingly, the corresponding  $\nu$  fluxes are estimated and compared with those calculated in the framework of some astrophysical models involving UHECR.

## 2 The neutrino induced flux

Let's be  $L_\gamma^*(\epsilon_\gamma, r) = dN_\gamma/dt d\epsilon_\gamma$  the photon spectral luminosity of the AGN measured in the source frame for a photon energy  $\epsilon_\gamma$  at a distance  $r$  from the core. Let's also assume that the gas and dust of the host galaxy are found in the form of protons and that their kinetic energies are negligible in comparison with the energies of the gamma-rays (supposition that can work for the hot, warm and cold gasses of the interstellar medium<sup>2</sup>).

In this way, the neutrino spectral luminosity,  $L_\nu(\epsilon_\nu)$  induced by the interaction of the gamma-photons with the intergalactic material of the galaxy on their way out along the direction of the observer is given by

$$L_\nu(\epsilon_\nu)d\epsilon_\nu = \int_0^{r_f} \int_{\epsilon_{\gamma,i}}^{\epsilon_{\gamma,f}} \rho_H(r) \sigma_{\gamma P}(\epsilon_\gamma) Y^{\gamma P \rightarrow \nu}(\epsilon_\gamma, \epsilon_\nu) L_\gamma^*(\epsilon_\gamma, r) d\epsilon_\gamma dr, \quad (1)$$

where  $\rho_H$  is the density of target protons at the distance  $r$ ,  $\sigma_{\gamma P}$  is the  $\gamma P$  cross section at a photon energy  $\epsilon_\gamma$  and  $Y^{\gamma P \rightarrow \nu}(\epsilon_\gamma, \epsilon_\nu)$  is the neutrino yield, which is defined as the number of  $\nu$ 's with energy in the interval  $d\epsilon_\nu$  around  $\epsilon_\nu$  produced by a photon with energy in the range  $[\epsilon_\gamma, \epsilon_\gamma + d\epsilon_\gamma]$  after a collision with a proton at rest. Energy losses of the parent particles in the  $\nu$ -production chain have been neglected.

Since,  $L_\gamma^*(\epsilon_\gamma, r)$  is unknown at the core of the AGN, the gamma-ray luminosity at source derived from Earth observations,  $L_\gamma(\epsilon_\gamma)$ , will be used instead in equation (1). Note that by doing so the estimated  $\nu$  flux could be lower than the real one, since the actual  $\gamma$ -ray

---

<sup>1</sup>The exact position of the high-energy source inside active galaxies is still an open problem. One candidate is the core of AGN's. In fact, multi-wavelength observations of M87 point out that the TeV gamma-ray production site could be located at the nucleus of its AGN [3].

<sup>2</sup>For example, the temperature of the gas supply for the central engine of some AGN's has been estimated to be of the order of keV [20, 21, 22], in such a medium, the mean kinetic energy expected for protons is roughly of the same order of magnitude, which results to be small in comparison with the gamma energies considered in this work ( $\epsilon_\gamma > 10^{-0.8}$  GeV).

luminosity could be bigger than  $L_\gamma(\epsilon_\gamma)$  at the interior of the AGN [23]. Now, by using the above approximation, equation (1) is reduced to the following expression:

$$L_\nu(\epsilon_\nu)d\epsilon_\nu = \Sigma_H \int_{\epsilon_{\gamma,i}}^{\epsilon_{\gamma,f}} \sigma_{\gamma P}(\epsilon_\gamma) Y^{\gamma P \rightarrow \nu}(\epsilon_\gamma, \epsilon_\nu) L_\gamma(\epsilon_\gamma) d\epsilon_\gamma, \quad (2)$$

with

$$\Sigma_H = \int_0^{r_f} \rho_H(r) dr. \quad (3)$$

Here,  $\Sigma_H$  is the column density of target protons along the line of sight from  $r = 0$  up to  $r_f$ , which corresponds to the size of the halo of the active galaxy. Integration limits for the energy parameters are defined as follows:  $(\epsilon_{\gamma,i}, \epsilon_{\gamma,f}) = (10^{-0.8} \text{ GeV}, 10^6 \text{ GeV})$  and  $(\epsilon_{\nu,i}, \epsilon_{\nu,f}) = (10^{-5} \text{ GeV}, 10^6 \text{ GeV})$ . The lower limit on the gamma-energies is set just at the threshold for pion photoproduction,  $\epsilon_{\gamma,th} = m_\pi(m_\pi c^2 + 2m_p c^2)/2m_p \approx 10^{-0.8} \text{ GeV}$  [24]. Meanwhile, the upper limit is fixed at  $10^6 \text{ GeV}$ , considering that the gamma-ray emission could be of leptonic origin and therefore that it could have a cut at the high-energy regime, somewhere around  $10^2 \text{ TeV}$  (see, for example, [25]).

The flux of neutrinos at Earth is estimated from the  $\nu$  luminosity of the active galaxy by means of the formula

$$\Phi_{\nu+\bar{\nu}}(\epsilon'_\nu) = \frac{(1+z)^2}{4\pi D_L^2} \cdot L_{\nu+\bar{\nu}}(\epsilon_\nu) \quad (4)$$

where  $z$  is the redshift of the galaxy and  $\epsilon'_\nu = \epsilon_\nu/(1+z)$  is the neutrino energy after redshift energy losses<sup>3</sup>.  $D_L$  is the luminosity distance to the source, which is defined as

$$D_L(z) = (1+z) \int_0^z c dz/H(z). \quad (5)$$

Here,  $c$  is the speed of light in vacuum and  $H(z)$  is the Hubble parameter at redshift  $z$ . For a cosmological scenario dominated by vacuum energy, with  $\Omega_\Lambda = 1 - \Omega_m$ ,

$$c/H(z) = (c/H_0)[1 - \Omega_m + \Omega_m(1+z)^3]^{-1/2}. \quad (6)$$

Along this paper, the following parameters will be used:  $\Omega_\Lambda = 0.74$  and  $c/H_0 = 1.28 \times 10^{28} \text{ cm}$  [26].

For the final fluxes of individual  $\nu$  flavors, neutrino oscillations will be taken into account [27]. That implies that after a long way to the Earth, neutrinos of different types will be present in the total flux in a  $(\nu_e + \bar{\nu}_e):(\nu_\mu + \bar{\nu}_\mu):(\nu_\tau + \bar{\nu}_\tau) = 1 : 1 : 1$  ratio.

### 3 Gamma ray luminosities

Several gamma-ray observatories have measured the differential photon spectra of Centaurus A and M87 in the MeV-TeV regime. For Centaurus A, measurements of the  $\gamma$ -ray flux in the interval  $0.1 - 1 \text{ GeV}$  have been performed with the EGRET detector on board of the Compton Gamma-Ray Observatory [4, 5], while in the  $0.1 - 30 \text{ GeV}$  energy range, data has been collected with the *Fermi*-LAT instrument [6]. Besides in the very high-energy region ( $\epsilon'_\gamma > 100 \text{ GeV}$ ), data has been registered with the telescopes of the H.E.S.S. experiment [7].

---

<sup>3</sup>Primed quantities are measured at Earth.

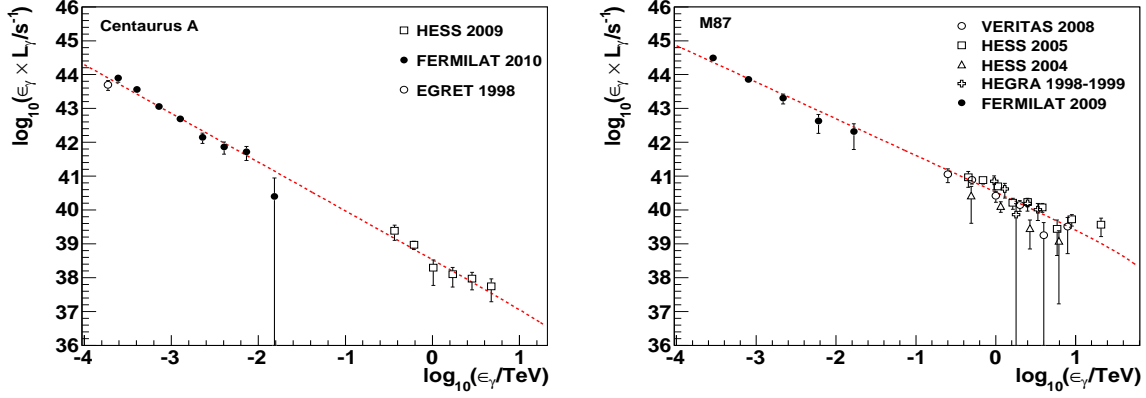


Figure 1: Photon spectral luminosities for Centaurus A (left) and M87 (right) derived from  $\gamma$ -ray measurements (data points) performed with different experiments (see text). The results of the fits with formula (8) are shown in each case (segmented lines).

In case of M87, its gamma-ray flux has been measured with the *Fermi*-LAT telescope in the range from 0.2 to 32 GeV and with HEGRA [8], HESS [9] and VERITAS [10] in the energy regime of 0.1 – 30 TeV.

Using the above observational data, the  $\gamma$  luminosities of the sources can be easily estimated. Let's be  $\Phi_\gamma(\epsilon'_\gamma) = dN_\gamma/dt'dA'd\epsilon'_\gamma$  the differential photon spectrum (in units of photons per unit time, unit area and interval of energy) detected at Earth from the active galaxy. Assuming a steady and isotropic emission, the photon spectral luminosity of the AGN is calculated by using

$$L_\gamma(\epsilon_\gamma) = 4\pi D_L^2 \cdot \frac{\Phi_\gamma(\epsilon_\gamma)}{(1+z)^2} \cdot e^{\tau(\epsilon_\gamma, z)}, \quad (7)$$

where corrections for both adiabatic energy losses due to the redshift and attenuation due to interactions with the background radiation are considered. The latter is done introducing the exponential term, where the parameter  $\tau(\epsilon_\gamma, z)$  appears. Here,  $\tau$  represents the  $\gamma\gamma$  optical depth for a photon traveling from the source with initial energy  $\epsilon_\gamma$ . The values used for  $\tau$  were taken from reference [28].

Photon spectral luminosities of Centaurus A and M87 at source, multiplied by  $\epsilon_\gamma$ , as derived from experimental data are presented in figure 1. Along the plots, individual fits using a power-law function with a cut-off at high-energies,

$$L_\gamma^{\text{fit}}(\epsilon_\gamma) = b \cdot \left[ \frac{\epsilon_\gamma}{\text{TeV}} \right]^a \cdot e^{-(\epsilon_\gamma/10^2 \text{ TeV})}, \quad (8)$$

are presented. The cut in expression (8) is introduced to model a  $\gamma$ -ray flux of leptonic origin. In the above equation,  $a$  and  $b$  stand for the fit parameters. The results of the fit are shown in table 1. Formula (8) will be employed in expression (2), when calculating the  $\nu$  luminosities.

By integrating  $L_\gamma(\epsilon_\gamma)$ , the integral luminosity,  $\mathcal{L}_\gamma$ , is obtained. Using equation (8) along with the parameters of table 1, a value of  $\mathcal{L}_\gamma(\epsilon_\gamma > 100 \text{ MeV}) = 7.2 \times 10^{40} \text{ erg} \cdot \text{s}^{-1}$  is derived for NGC 5128 and,  $\mathcal{L}_\gamma(\epsilon_\gamma > 100 \text{ MeV}) = 1.1 \times 10^{42} \text{ erg} \cdot \text{s}^{-1}$ , for M87. The integral luminosity of M87 results to be almost one order of magnitude bigger than that of Centaurus A.

## 4 Gas and dust distributions of the galaxies

### 4.1 Centaurus A

Due to its proximity to Earth, Centaurus A has been well studied in the literature (see for example, the reviews [29, 30]). To calculate  $\Sigma_H$  along the line of sight a simple model is built based on the observational data. The main parameters are presented in table 2.

The most prominent features of Centaurus A are the nuclear region, the circumnuclear disk, the dust lane, the jets and the halo [29, 30]. All of them, but the jet structures, are included in the model, since the jets do not lie along the line of sight.

In this model of Centaurus A, the VLBI radio core [31] is assumed to be the source of the  $\gamma$  radiation. This supposition is not yet confirmed, but it is still consistent with observations [7, 6]. A source with radius  $R = 0.01$  pc (corresponding to the upper limit on the size of the radio source established by VLBI observations [31]) and density  $n_H \approx 10^6 \text{ cm}^{-3}$  (as derived in [32] assuming free-free absorption in the core of Centaurus A and using data from mm and X-ray observations) will be considered in this paper.

X-ray observations of the nucleus of Centaurus A reveal the presence of two spectra with different degrees of nuclear absorption [33]. The spectra could be associated either with the emission of a single X-ray source attenuated by different components of a strong absorber [33, 34, 35] or with the combined emission from the accretion disk and the pc-scale VLBI jet [22]. Here, the first scenario will be considered. In particular, it will be assumed that the absorber is in the form of a cold cloud entirely surrounding the core [36] characterized by a column density with weighted-mean of  $2.4 \times 10^{23} \text{ cm}^{-2}$  (best-fit model from [33]). For simplicity, a cloud with uniform density and radius  $R = 0.1$  pc (equivalent to the emission radius of the Fe  $K\alpha$  lines observed in the X-ray spectra, which seem to belong to the absorber [22]) will be employed in the calculations.

Along the central region of Centaurus A, gas and dust seem to be organized in the form of a warped disk [2, 37], which can be modeled by means of tilted rings with different position ( $PA$ ) and inclination ( $i$ ) angles (see [38] and references therein). These tilted rings will be incorporated into the models of the nuclear disk [39] and the dust lane [29]. However, for the circumnuclear disk, only a single ring will be used [40].

The nuclear disk will be considered as the result of individual tilted rings distributed between  $r = 0.1$  and 40 pc. The position ( $PA$ ) and inclination ( $i$ ) angles of the rings are taken from the SINFONI data [39]. Since observations in [39] are reported only for  $r = 0.824 - 31.3$  pc, for those nuclear rings lying outside the previous range the angular parameters will be kept constant. An aspect ratio  $k(R) = h(R)/R = 0.5$  is assumed for the rings, where  $h(R)$  is the thickness as a function of the cylindrical radius,  $R$ .

For the circumnuclear disk a single ring with external radius  $R = 200$  pc, thickness of 80 pc

Table 1: Values of the fit parameters  $a$  and  $b$  of formula (8) for Centaurus A and M87.

AGN	$\log_{10}[b/\text{s}^{-1} \cdot \text{TeV}^{-1}]$	$a$
Centaurus A	$38.53 \pm 0.09$	$-2.44 \pm 0.03$
M87	$40.53 \pm 0.03$	$-2.08 \pm 0.02$

Table 2: Extension and density distribution of the gas structures in the model of Centaurus A. Here,  $R$  represents the cylindrical radius and  $r$ , the spherical one.

Structure	$R$ [pc]	$n_H$ [cm $^{-3}$ ]
Core	0.01	$10^6$
X-ray absorber	0.01 – 0.1	$8.6 \times 10^5$
Nuclear disk	0.1 – 40	$3.4 \times 10^2$
Circumnuclear disk	40 – 200	$(5.5 \times 10^5)/r^2$
Dust lane	$(0.8 - 7) \times 10^3$	$(3.6 \times 10^{13})/r^4$
ISM and halo	$35 \times 10^3$	$4 \times 10^{-2}[1 + (r/500 \text{ pc})^2]^{-0.6}$

and internal radius  $R = 40$  pc will be assumed, in accordance with the studies of  $CO(1 - 0)$  absorption and  $H_2$  emission against the nucleus [40]. The disk with  $PA = 155^\circ$  and  $i = 70^\circ$  is considered to have a gas mass of  $\sim 10^7 M_\odot$  distributed in the form  $n_H \sim r^{-2}$ , where  $r$  is the spherical radius [40]. This expression will be extrapolated up to the region  $r < 40$  pc in order to find the density inside the nuclear disk.

The dust lane, extended from  $r = 800$  pc [29] up to 7 kpc [30], will be also described with the tilted ring model [29, 41, 42]. The position and inclination angles of the rings are taken from references [2, 38, 43] and the disk aspect ratio ( $k(R) = h(R)/R = 0.1 \cdot [R/824 \text{ pc}]^{0.9}$ ), from [2]. A dusty disk with a mass of the order  $1.3 \times 10^9 M_\odot$  [30] and a density distribution of the form  $r^{-4}$  [2, 42] will be assumed in this work.

Finally, the last structure to include is the halo, which has a radius of at least  $r_f = 35$  kpc according to XMM-Newton observations [44]. It has been found from studies of NGC 5128 performed with the Chandra and XMM-Newton, that the density profile of the halo for  $r \lesssim 10$  kpc can be very well represented by a beta model for distances,  $n_H = n_0[1 + (r/r_0)^{-1.5\xi}]$ , with  $n_0 = 4 \times 10^{-2} \text{ cm}^{-3}$ ,  $r_0 = 500$  pc and  $\xi = 0.40 \pm 0.04$  [44]. Along the paper, this expression will be used to infer the density distribution of the interstellar medium (ISM) and the material in the halo up to a distance of 35 kpc from the AGN's core.

By integrating numerically the density of target protons along the line of sight, the corresponding column density is found and amounts to  $4.4 \times 10^{23} \text{ cm}^{-2}$ .

## 4.2 M87

Astronomical observations show the presence of a core [45], a nuclear disk [46], a kpc jet [47, 48] and a halo [49, 50, 51] in M87. As it was the case for Centaurus A, only the jets will be left out of the present model of M87. The principal structures involved in the model, as well as their densities and sizes, are summarized in table 3.

The source of gamma rays will be located at the core of the radio galaxy in the model. In fact, results of the 2008 multi-wavelength campaign on M87 show evidence in favor of a correlation between the radio core and the TeV emissions [3]. Following the model proposed in [11] to explain the *Fermi*-LAT MeV/GeV observations, a gamma source with a radius of  $r_1 = 4.5$  mpc is assumed. Since the density of the source is uncertain, the value  $n_H = 10^6 \text{ cm}^{-3}$  will be used, which is in agreement with limits presented in [52] and estimations from [53] (based on observations of UV and optical emission lines measured with instruments of the Hubble Space Telescope).

Table 3: Extension and density distribution of main gas structures in the model of M87. Here,  $R$  represents the cylindrical radius and  $r$ , the spherical one.

Structure	$R$ [pc]	$n_H$ [cm $^{-3}$ ]
Core	0.0045	$10^6$
Nuclear disk	100	3.24
Halo	$260 \times 10^3$	$4.2 \times 10^{-2} [1 + (r/7.87 \text{ kpc})^2]^{-0.654}$

The nuclear disk of M87 will be modeled using a thin disk with a radius  $r = 100$  pc [46, 54] and thickness of 10 pc (as in reference [55]). This is just a simplified picture, since the nuclear disk has a more complex structure. Observations with the Hubble Space Telescope show spiral arms in the nuclear disk, which are apparently connected with 1 kpc-scale filaments of gas [46, 54]. The position and inclination angles of the nuclear disk are  $PA = 6^\circ$  and  $i = 35^\circ$ , respectively [56]. The mean surface density of the disk in the model will be  $\Sigma_H = 10^{20} \text{ cm}^{-2}$ , which is within the range of values derived from the results of different studies [53, 55, 57].

The density profile of the ISM and halo of M87 will be described with the beta model of reference [58],  $n_H = n_0 [1 + (r/r_0)^{-1.5\xi}]$ , where  $n_0 = 4.2 \times 10^{-2} \text{ cm}^{-3}$ ,  $r_0 = (7.87 \pm 1.36) \times 10^3 \text{ pc}$  and  $\xi = 0.436 \pm 0.008$ . The parameters of the above function were obtained from fits to the X-ray data from the Einstein observatory of the hot halo of M87 [58]. The radius of the halo will be set at  $r_f = 260 \text{ kpc}$ , distance at which the measured gas is still associated with M87 [58].

Using the model described in this section, the column density of target protons in M87 along the line of sight of the active galaxy is estimated. The result is  $\Sigma_H = 2.90 \times 10^{21} \text{ cm}^{-2}$ , two orders of magnitude lower than that for Centaurus A.

## 5 The $\gamma P$ hadronic cross section and the neutrino yields

The total  $\gamma P$  hadronic cross section above  $\sqrt{s} = 5 \text{ GeV}$  is evaluated with the parameterized formula of references [26, 59]:

$$\sigma_{\gamma P} = \delta \cdot Z + \delta \cdot B \log^2(s/s_0) + Y(s_1/s)^\eta, \quad (9)$$

where  $\sqrt{s}$  is the center-of-mass energy and  $\sqrt{s_1}$  is an energy scale fixed at 1 GeV.  $\delta = 0.00308$ ,  $Z = 35.45 \text{ mb}$ ,  $B = 0.308 \text{ mb}$ ,  $Y = 0.0320 \text{ mb}$  and  $\eta_1 = 0.458$ , while  $\sqrt{s_0} = 5.38 \text{ GeV}$  [26]. These parameters were obtained by the COMPETE Collaboration by means of a global fit to current accelerator data with  $\sqrt{s} \geq 5 \text{ GeV}$  [59].

For center-of-mass energies inside the interval  $\sqrt{s} = 1 - 5 \text{ GeV}$  the total hadronic cross section is calculated by interpolating the  $\sigma_{\gamma P}$  data presented in [26].

On the other hand, neutrino yields are obtained using the Monte Carlo program SOPHIA 2.01 [60]<sup>4</sup>. The procedure is as follows: Gamma-photons and neutrino energy ranges are divided in several intervals (in logarithmic scale). Then collisions of gamma-photons with energy  $\log_{10} \epsilon_{\gamma,i}$  against protons at rest are simulated with SOPHIA and the number of neutrinos,  $n_{ij}$ , produced with energy in the bin  $\log_{10} \epsilon_{\nu,j}$  is counted. Neutrino yields,  $Y_{ij}^{\gamma P \rightarrow \nu}$ ,

<sup>4</sup>Simulations with PYTHIA 6.4 [61] were also used to check out the results for the neutrino yields at high-energies. They gave also values of the same order of magnitude than those found with SOPHIA.

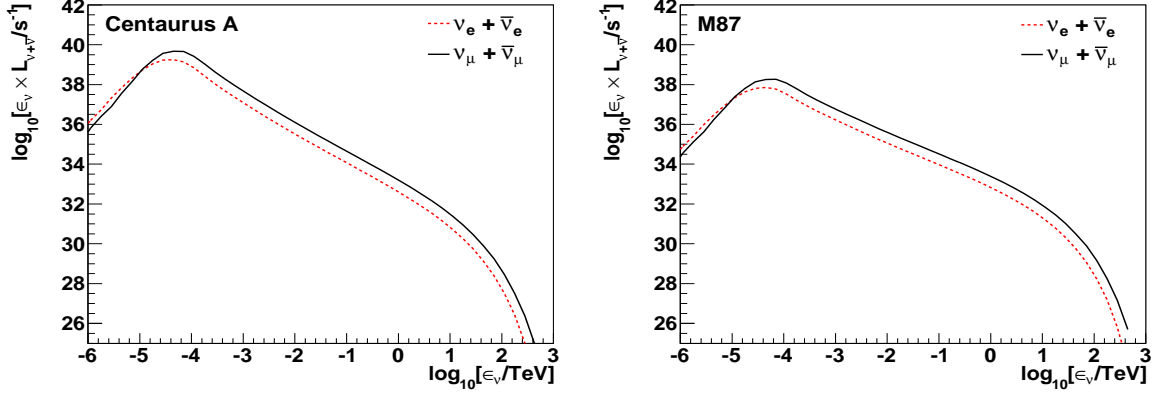


Figure 2: Electron (dotted line) and muon (solid line) neutrino luminosities expected from Centaurus A (left) and M87 (right) at source and produced by interactions of their own  $\gamma$  radiation with the gas and dust in the corresponding galaxies.

are estimated averaging  $n_{ij}$  over all events induced by photons with energy  $\log_{10} \epsilon_{\gamma,i}$ . The  $\nu$  yields were calculated only for electron and muon neutrinos, since simulations show that the tau neutrino production in  $\gamma P$  collisions is negligible in the energy range under consideration.

## 6 Results

Electron and muon neutrino luminosities at source for NGC 5128 and M87 are shown in figure 2. They are restricted at low- and high-energies by the pion photoproduction energy threshold and the exponential energy cut imposed on the  $\gamma$ -ray luminosities, respectively. Inbetween,  $\nu$  luminosities follow a simple power-law only interrupted at low-energies ( $\epsilon_\nu \sim 10^{-4}$  TeV) by a small bump that emerges as a result of the enhancement of the cross section due to the production of hadronic resonances in  $\gamma P$  interactions.

From data presented in figure 2, integrated neutrino luminosities can be derived. They are found to be quite low. Integrating  $L_{\nu+\bar{\nu}}$  for energies above 100 MeV and summing for electron and muon neutrinos, in case of Centaurus A, the following value results  $\mathcal{L}_{\nu+\bar{\nu}}(\epsilon_\nu > 100 \text{ MeV}) = 1.04 \times 10^{36} \text{ erg} \cdot \text{s}^{-1}$ . Meanwhile, for M87, the value  $\mathcal{L}_{\nu+\bar{\nu}}(\epsilon_\nu > 100 \text{ MeV}) = 1.28 \times 10^{35} \text{ erg} \cdot \text{s}^{-1}$  is obtained. These integrated luminosities are from 5 to 7 orders of magnitude smaller than the ones corresponding to  $\gamma$ -rays.

In figure 3, the final neutrino fluxes (per flavor) arriving at Earth are presented and are compared with the 90% confidence level upper bounds obtained with the Antares[62], Amanda[63] and ICECUBE[64] detectors for the  $\nu$  fluxes from Centaurus A and M87. The difference between experimental bounds and expected values are too big, the latter ones are more than 6 orders of magnitude smaller than the experimental limits. Therefore, neutrinos from Centaurus A and M87 coming from interactions of their own  $\gamma$ -ray flux with the respective gas and dust could escape detection at the modern neutrino observatories.

In figure 3 (left panel), the expected  $\nu$  fluxes from Centaurus A from three different models involving cosmic rays are also shown for comparison. In all cases, the cosmic ray fluxes (composed by protons) are normalized using the data from the Pierre Auger observatory [12]. One model, due to Hylke et al., assumes that acceleration takes place at the jets [14]. The second model, worked out by Kachelriess et al., invokes cosmic ray acceleration close to



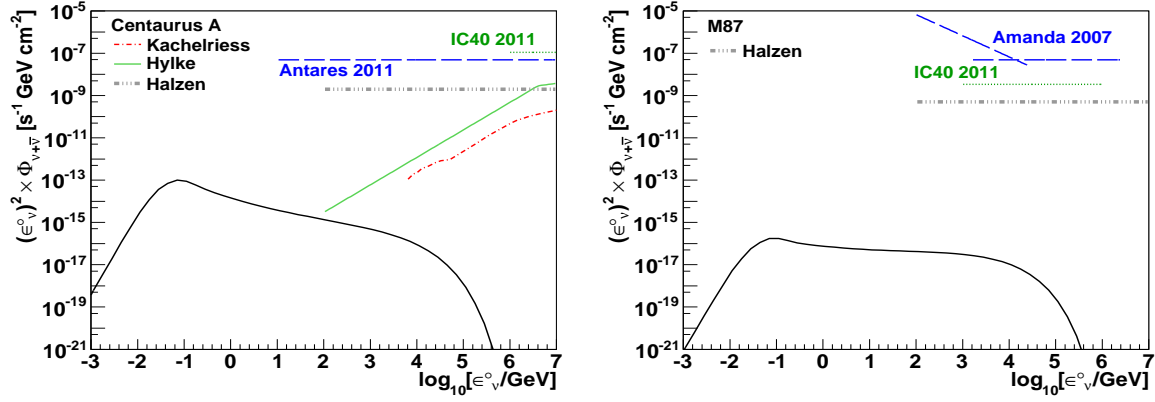


Figure 3: Neutrino and antineutrino fluxes expected from Centaurus A (left) and M87 (right) at Earth for each neutrino type. The flux is produced by interactions of their own  $\gamma$  radiation with the gas and dust at the sources. Neutrino oscillations are taken into account. Individual 90% C.L upper limits on the neutrino fluxes established with the Amanda [63], ICECUBE [64] and Antares [62] detectors for each galaxy are also shown. For M87, two different  $\nu$  limits from Amanda are presented (segmented lines). They were estimated assuming different spectral indices for the differential  $\nu$  flux:  $\gamma = -2$  and  $-3$  (horizontal and inclined lines, respectively) [63]. Finally, predictions for Centaurus A (Kachelriess [13], Hylke [14] and Halzen [15, 16]) and M87 (Halzen [15, 16]) based on different models involving cosmic rays are plotted.

the core (with spectral index  $\alpha = 2.7$ ) [13]. The last model, proposed in [15], uses also the  $\gamma$ -ray data from the HESS detector [65] to put an upper limit on the neutrino flux assuming a pionic origin of the TeV radiation. This limit is also applied in [16] to M87 (see right panel of figure 3) by noting that luminosities from Centaurus A and M87 are similar at TeV energies. It is clear from the above figure that at high-energies, relevant for neutrino astronomy ( $\epsilon_\nu \gtrsim 1$  TeV), neutrinos from the cosmic ray channel dominate over the modest contribution from  $\gamma P$  interactions studied in this paper.

## 7 Conclusions

The GeV-TeV gamma-ray flux detected from Centaurus A and M87 should be producing a feeble  $\nu$  flux arising from its photo-hadronic interactions with the material of the sources. Estimated  $\nu$  luminosities are from  $10^{-5}$  to  $10^{-7}$  times the corresponding luminosities for  $\gamma$ -rays, in case of Centaurus A and M87, respectively. For the simple models here analyzed, derived  $\nu$  fluxes are found to be  $E^2 \Phi_{\nu+\bar{\nu}} \lesssim 10^{-13} \text{ s}^{-1} \text{ GeV cm}^{-2}$ , i.e. more than 6 orders of magnitude below the upper experimental limits. That result implies that these fluxes could escape experimental detection at modern neutrino telescopes like ANTARES and ICECUBE. Estimations are still dependent on the real position of the  $\gamma$  ray source at the active galaxy and on the shape and magnitude of the  $\gamma$ -ray spectrum at the interior of the source, which are at the moment unknown.

# Acknowledgments

The author thanks R. Engel for his suggestions on the Monte-Carlo programs for photo-hadronic interactions. This work has been partially supported by the Coordinación de la Investigación Científica de la Universidad Michoacana.

# References

- [1] B.L. Fanaroff and J.M. Riley, MNRAS 167 (1974) 31P.
- [2] A. Quillen, ApJ 645 (2006) 1092.
- [3] The VERITAS Collaboration, the VLBA 43 GHz M87 Monitoring Team, the H.E.S.S. Collaboration and the MAGIC Collaboration, Science 325 (2009) 444, arXiv: 0908.0511.
- [4] H. Steinle et al., A&A 33 (1998) 97.
- [5] P. Sreekumar et al., Astrop. Phys. 11 (1999) 221.
- [6] A. A. Abdo et al., ApJ 719 (2010) 1433, arXiv: 1006.5463.
- [7] F. Aharonian et al., ApJ 695 (2009) L40, arXiv: 0903.1582.
- [8] Aharonian F. et al., ApJ 614 (2004) 897.
- [9] Aharonian F. et al., A&A 457 (2006) 899.
- [10] V.A. Acciari et al., ApJ 679 (2008) 397, arXiv: 0802.1951.
- [11] A. A. Abdo et al., ApJ 707 (2009) 55, arXiv: 0910.3565.
- [12] J. Abraham et al. (PAO Collaboration), Science 318 (2007) 939, arXiv: 0711.2256.
- [13] M. Kachelriess et al., New Journal of Physics 11 (2009) 065017.
- [14] B. Hylke et al., Phys. Rev., D78 (2008) 083009.
- [15] F. Halzen and A. O’Murchadha, arXiv: 0802.0887v2.
- [16] F. Halzen, arXiv: 1111.1131v1.
- [17] S. Razzaque et al., Phys. Rev. D 73 (2006) 103005.
- [18] C. D. Dermer and G. Menon, High Energy Radiation from Black Holes: Gamma Rays, Cosmic Rays, and Neutrinos, Princeton University Press, 2009.
- [19] H.Y. Chiu, R.C. Stabler, Phys. Rev. 122 (1961) 1317. V.I. Ritus, JETP 14 (1962) 915. G. Beaudet et al., Phys. Rev. 154 (1966) 1445.
- [20] S. W. Allen et al., Mon. Not. R. Astron. Soc. 372 (2006) 21.
- [21] D. A. Evans et al., ApJ 642 (2006) 96, arXiv:0512600.

- [22] D. A. Evans et al., *ApJ* 612 (2004) 786.
- [23] M. Kachelriess et al., *PASA* 27 (2010) 482-489.
- [24] R.J. Protheroe and P. A. Johnson, *Astrop. Phys.* 4 (1996) 253, arXiv: 9506119.
- [25] M. M. Reynoso, M. C. Medina, G. E. Romero, *A&A* 531 A30 (2011).
- [26] K. Nakamura et al. (Particle Data Group), Review of particle physics, *J. Phys. G* 37 (2010) 075021.
- [27] K. Nakamura and S.T Petcov, Neutrino Mass, mixing and oscillations, in: reference [26].
- [28] A. Franceschini et al., *A&A* 487, 837 (2008), arXiv: 0805.1841.
- [29] R. Morganti, *PASA* 27 (2010) 463, arXiv:1003.5568.
- [30] F.P. Israel, *Astron. Astrophys. Rev.* 8 (1998) 237.
- [31] K.I. Kellermann et al., *ApJ* 475 (1997) L93.
- [32] Z. Abraham et al., *Mon. Not. R. Astron. Soc.* 375 (2007) 171.
- [33] A. Markowitz et al., *ApJ* 665 (2007) 209.
- [34] T.J. Turner et al., *ApJ* 475 (1997) 118.
- [35] P.R. Wozniak, et al., *MNRAS* 299 (1998) 449.
- [36] S. Miyazaki et al., *Pbl. Astron. Soc. Japan* 48 (1996) 801.
- [37] A.D. Tubbs, *ApJ* 241 (1980) 969.
- [38] A.C. Quillen, *PASA* 27 (2010) 396, arXiv:0912.0632.
- [39] N. Neumayer et al., *ApJ* 671 (2007) 1329.
- [40] F.P. Israel et al., *A&A* 227 (1990) 342.
- [41] R.A. Nicholson et al., *ApJ* 387 (1992) 503.
- [42] A.C. Quillen et al., *ApJ* 391 (1992) 121.
- [43] D. Espada et al., *ApJ* 695 (2009) 116.
- [44] R. P. Kraft et al., *ApJ* 698 (2009) 2036.
- [45] M.H. Cohen et al., *ApJ* 158 (1969) L83.
- [46] H.C. Ford et al., *ApJ* 435 (1994) L27.
- [47] H.D. Curtis, *Pub. Lick. Obs.* 13 (1918) 31.
- [48] J. Biretta in: D. Burgarella et al. (Eds.), *Astrophysical Jets*, Cambridge University Press, (1994) 263. J.A. Biretta & W. Junor, *Proc. Natl. Acad. Sci.* 92 (1995) 11364.
- [49] R. Malina et al., *ApJ* 209 (1976) 678.

- [50] E.J. Schreier et al., ApJ 261 (1982) 42.
- [51] C.L. Sarazin, X-ray Emission from Clusters of Galaxies, Cambridge Astrophysics Series, Cambridge University Press, 1988.
- [52] A. Neronov & F.A. Aharonian, ApJ 671 (2007) 85.
- [53] B.M. Sabra et al., ApJ 584 (2003) 164.
- [54] H. Ford & Z. Tsvetanov, Lecture Notes in Physics 530 (1999) 278.
- [55] J.C. Tan et al., ApJ 689 (2008) 775.
- [56] Z.I. Tsvetanov et al., Proceedings of the M87 Workshop, Ringberg castle, Germany (1998) 15 arXiv: 9803178.
- [57] M.A. Dopita et al., ApJ 490 (1997) 202.
- [58] D. Fabricant & P. Gorenstein, ApJ 267 (1983) 535.
- [59] J.R. Crudell et al. (COMPETE Collab.), Phys. Rev. D65 (2002) 074024.
- [60] A. Mücke, R. Engel, J.P. Rachen, R.J. Protheroe, and T. Stanev, Comp. Phys. Commun. 124 (2000) 290, arXiv: 9903478.
- [61] T. Sjöstrand et al., JHEP05(2006)026.
- [62] S. Adrián-Martínez et al., ApJL 743 (2011) L14, arXiv:1108.0292v1.
- [63] M. Ackermann, Astrophys. Space. Sci. 309 (2007) 421.
- [64] R. Abbasi et al., ApJ 732 (2011) 18.
- [65] F. Aharonian et al., A&A. 441 (2005) 465.